New Journal of Physics
The open-access journal for physics

Elastic properties of graphene suspended on a polymer substrate by e-beam exposure

Floriano Traversi[1], Francisco Javier Gúzman-Vázquez[2], Laura Giorgia Rizzi[1], Valeria Russo[3], Carlo Spartaco Casari[3], Cristina Gómez-Navarro[2,4] and Roman Sordan[1,4]

[1] L-NESS, Department of Physics, Politecnico di Milano, Polo di Como, Via Anzani 42, 22100 Como, Italy
[2] Departamento de Física de la Materia Condensada, Universidad Autónoma de Madrid, 28049 Madrid, Spain
[3] Department of Energy, Politecnico di Milano, Via Ponzio 34/3, 20133 Milano, Italy
and
Center for Nano Science and Technology of IIT@PoliMI, Via Pascoli 70/3, 20133 Milano, Italy
E-mail: cristina.gomez@uam.es and roman.sordan@como.polimi.it

New Journal of Physics **12** (2010) 023034 (8pp)
Received 9 October 2009
Published 24 February 2010
Online at http://www.njp.org/
doi:10.1088/1367-2630/12/2/023034

Abstract. A method for fabricating multiple free-standing structures on the same sheet of graphene is demonstrated. Mechanically exfoliated mono- and bilayer graphene sheets were sandwiched between two layers of polymethyl-methacrylate. Suspended areas were defined by e-beam exposure allowing precise control over their shape and position. Mechanical characterization of suspended graphene sheets was performed by nanoindentation with an atomic force microscopy tip. The obtained built-in tensions of 12 nN are significantly lower than those in suspended graphene exfoliated on an SiO_2 substrate, and therefore permit access to the intrinsic properties of this material system.

[4] Author to whom any correspondence should be addressed.

Contents

1. Introduction

Graphene, a recently isolated [1] one-atom-thick crystal of carbon atoms arranged in a honeycomb lattice, has attracted a great deal of interest during the past few years owing to its remarkable electronic [2] and mechanical [3] properties. The unique combination of very high carrier mobility [4], high intrinsic strength [3], and very low mass of suspended graphene sheets makes graphene ideal as a main building block of advanced nanoelectromechanical systems (NEMS) [5]. Graphene NEMS operate as highly sensitive resonators [6], with resonant frequencies in the gigahertz range [7], and exhibit a new class of nanoscale vibrations [8]. Most of the investigated NEMS have so far been fabricated by mechanical exfoliation of graphite. Owing to the very small probability of obtaining monolayer graphene in this process ($\sim$1 monolayer graphene per 3 mm^2), large arrays of pits or trenches were pre-patterned on the substrates. Such a large etched area covers most of the chip and therefore prevents the integration of suspended graphene with other devices. This problem can be mitigated by selective suspension of graphene sheets in which the underlying oxide is etched by buffered hydrofluoric acid (BHF) only below selected graphene sheets [9]. However, wet etching is an isotropic process and the shape of the underetched area cannot be controlled. In addition, the surface tension associated with this process leads to the collapse of suspended sheets if the samples have not been critical-point dried [4, 9, 10]. Here we demonstrate a simple method for the fabrication of multiple suspended devices on the same sheet of graphene. The method does not require critical-point drying and provides full control over the shape and position of the suspended areas. This was achieved by suspending mono- and bilayer graphene sheets on a polymer substrate in which suspended areas were defined by e-beam exposure. The sheets are found to have much lower built-in tension than sheets exfoliated on an SiO_2 substrate, which allows access to the intrinsic properties of suspended graphene and provides predictable and reproducible resonant frequencies.

2. Experimental details

The fabrication procedure is schematically depicted in figure 1. In the first step, e-beam-resist polymethyl-methacrylate (PMMA) dissolved in chlorobenzene was spin coated on a highly doped Si substrate with 300 nm of thermally grown dry SiO_2 on top. Different types of PMMA were used, resulting in layer thicknesses between 90 and 250 nm after baking. Graphene sheets were deposited on PMMA by mechanical exfoliation [1] of highly oriented pyrolitic graphite (figure 1(a)). Possible mono- and bilayer graphene sheets were scanned by atomic force microscopy (AFM) after they were identified by optical microscopy. While monolayer graphene deposited on an SiO_2 substrate usually exhibits a thickness of $\sim$1.2 nm under AFM, monolayer

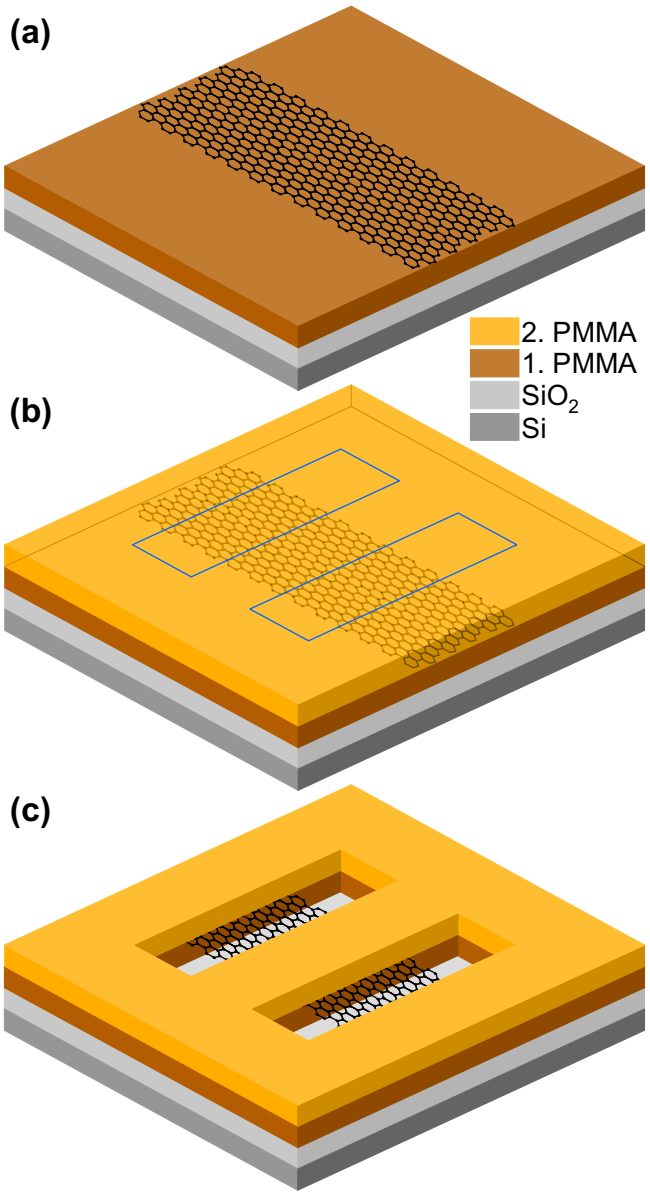

Figure 1. Schematic of the fabrication steps for suspending graphene on a polymer substrate. (a) Graphene is deposited on a polymer (e-beam-resist PMMA) previously spin coated on a highly doped Si substrate with an SiO_2 top layer. (b) A second polymer layer is deposited on top of the graphene. Areas within the blue rectangles are subsequently exposed to the e-beam. (c) Suspended graphene is obtained after exposed areas are developed.

graphene deposited on PMMA exhibited a thickness of ∼1.6 nm. In the second step, the second PMMA layer was spin coated on the top (figure 1(b)). After baking, rectangular areas across the sheets were exposed to the e-beam. In the third step, PMMA was developed by a standard methyl isobutyl ketone/isopropyl alcohol developer, resulting in windows in the PMMA layer that cross each graphene sheet, leaving parts of the graphene sheet suspended between the PMMA layers

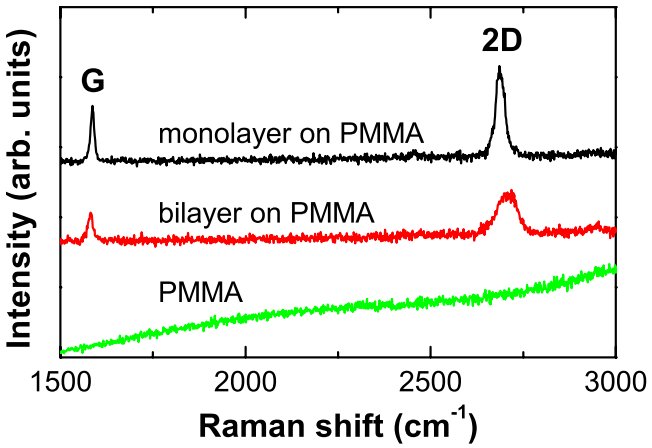

Figure 2. Raman spectra collected at 514.5 nm of monolayer (black) and bilayer (red) graphene deposited on a PMMA substrate. The spectrum of a bare PMMA substrate is shown in green.

(figure 1(c)). The windows were made wider than the graphene sheet in order to develop the bottom PMMA layer from the sides. A much longer ($\sim 10\times$) development time was required than in the case of a double PMMA layer without embedded graphene, as the developer had to penetrate the bottom layer along the windows.

The exact number of graphene layers deposited on the first PMMA layer was determined by Raman spectroscopy. Figure 2 shows Raman spectra of mono- and bilayer graphene exfoliated on a PMMA substrate. No significant contribution from the substrate, the spectrum of which is also shown in the same figure, is observed in the graphene spectra. The single Lorentzian and very intense second-order band (marked by 2D) allow a monolayer sheet to be identified. The 2D peak exhibits the same evolution with the number of layers as in Raman spectra of graphene deposited on a conventional SiO_2 substrate [11]. The influence of the underlying PMMA substrate was observed only when the first PMMA layer was very thick (>300 nm), but even in this case the typical shape of the graphene Raman bands was still clearly visible.

A fabricated suspended graphene device is shown in figure 3. The graphene sheet was suspended over five 1.2-μm-wide rectangular windows. The sheet consists of monolayer (the first two windows on the right-hand side) and bilayer parts (the other three windows). The shape and position of the windows were defined by e-beam exposure after the sheet was initially characterized by AFM. The windows have well-defined vertical sidewalls as the developer dissolves only the exposed parts of the PMMA layers. The windows are 450 nm deep and the sheet is freely suspended 200 nm above the surface of the SiO_2 layer. Critical-point drying was not needed in fabrication because the surface tension of the developer is ~ 4 times less than that of BHF/H_2O. Each of the suspended parts of the sheet forms a double-clamped beam whose length is equal to the width of the corresponding window. Once the structure was fabricated, the exact length l and width w of each beam was determined by AFM. Non-contact mode was used in order to avoid any damage to the sheet.

Mechanical characterization of the fabricated suspended graphene sheets was performed under ambient conditions. Deflection of the AFM tip z_{tip} was measured while the tip was lowered by z_{piezo}, indenting the center of the suspended area. The force constant of the tip

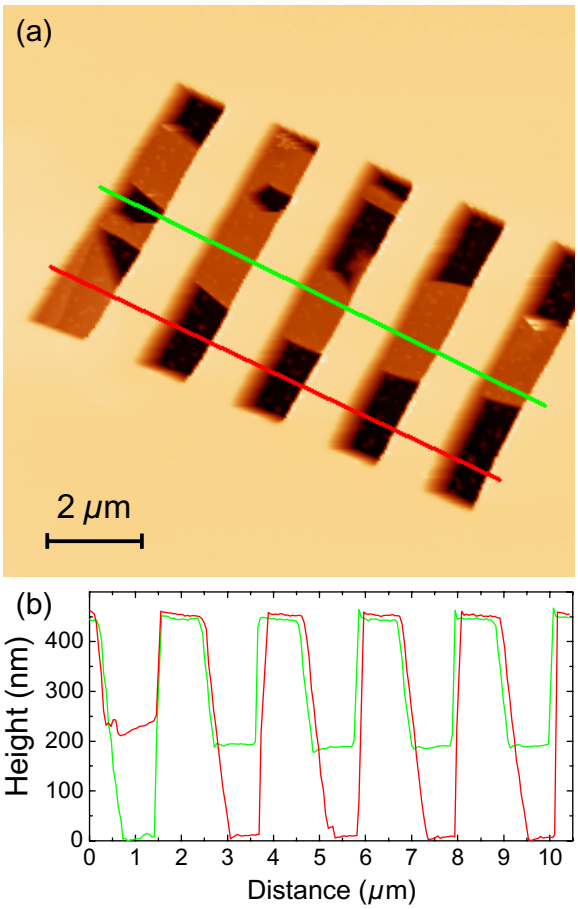

Figure 3. A graphene sheet suspended over five PMMA windows. (a) AFM image of the device. (b) Height profiles of the device along green and red sections in (a). The thicknesses of the bottom and top layers are 200 and 250 nm.

k_{tip} was calibrated by Sader's method [12], allowing calculation of the force exerted on the tip in the linear regime (small deflections) as $F = k_{\mathrm{tip}} z_{\mathrm{tip}}$. Several force–distance curves F versus z_{piezo} were acquired in each suspended structure (one is shown in red in figure 4(a)). Similar curves on a hard SiO_2 substrate (for which $z_{\mathrm{piezo}} = z_{\mathrm{tip}}$) were used to calibrate the applied force F and deflection of the sheets $z = z_{\mathrm{piezo}} - z_{\mathrm{tip}}$ (figure 4(a)). The elastic constant of the devices was then calculated as $k = \mathrm{d}F/\mathrm{d}z$ in the low deformation regime, where $F(z)$ is linear and the sheet is in the pure bending regime (figure 4(b)). In addition, no dynamic effects were found for indentation speeds of 10–500 nm s^{-1}.

3. Results and discussion

The elastic constant k of the suspended graphene sheet in the linear regime can be related to the elastic modulus E of graphene by the expression valid for a double-clamped beam under point load as [13]

$$k = 32Ew(t/l)^3 + 17T/l, \tag{1}$$

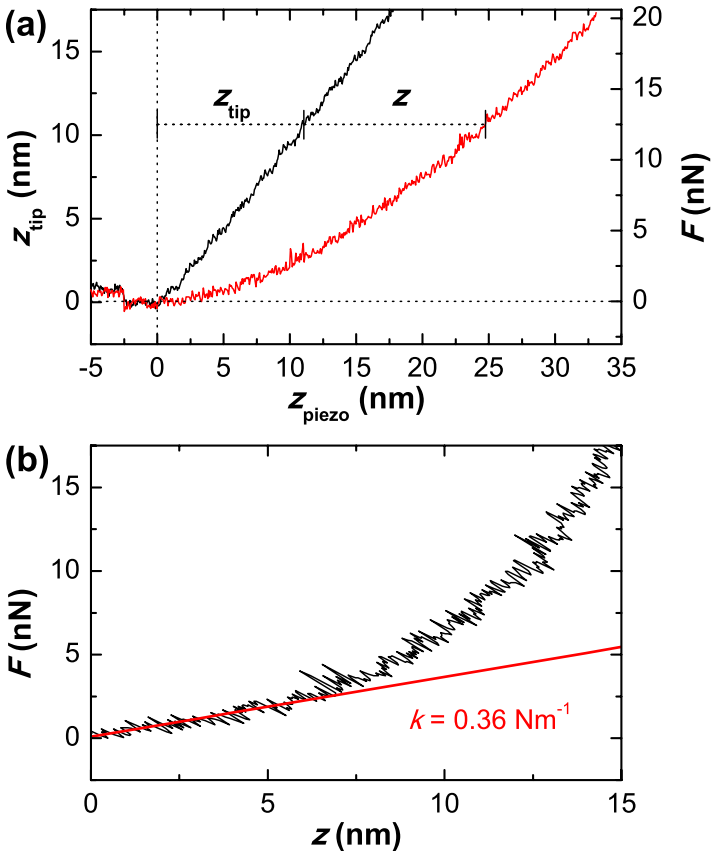

Figure 4. Force–distance curves measured by a tip with an elastic constant $k_{\mathrm{tip}} = 1.21\,\mathrm{N\,m^{-1}}$. (a) A curve measured on a hard substrate (black) and suspended graphene sheet (red). The difference in z_{piezo} of the curves at a fixed force F is equal to the displacement z of the sheet. (b) Force exerted on the sheet as a function of the displacement of the sheet. The elastic constant k of the sheet is calculated as the slope of the force–displacement curve in the linear regime.

where t is the thickness of the sheet ($t = 0.34\,\mathrm{nm}$ for monolayer graphene and $t = 0.68\,\mathrm{nm}$ for bilayer graphene) and T is the built-in tension of the sheet. In the limit of vanishing tension $T \to 0$ a linear scaling of elastic constant k with $w(t/l)^3$ is expected. Experimental data for k versus $w(t/l)^3$ are plotted in figure 5(a) for 13 different suspended mono- and bilayer graphene sheets. The pronounced scatter exhibited in this plot indicates a non-negligible built-in tension, $T > 0$. These tensions are regularly present in most NEMS and result from the fabrication procedures [5]. Particularly, for graphene, they have been attributed to forces applied on the sheet during the mechanical exfoliation process, which stretches the sheet on the substrate.

The tension can be determined by rewriting equation (1) as $E_k = E + (17/32)Tl^2/(wt^3)$ where $E_k = kl^3/(32wt^3)$. Experimental data for E_k versus $l^2/(wt^3)$ are plotted for the investigated sheets in figure 5(b). A slope of the linear fit of the plotted data reveals a built-in tension of $T = 12\,\mathrm{nN}$. However, the scatter that is also visible in this plot has a strong influence on the intercept in the linear fit, which indicates a variation in E from sheet to sheet. The elastic modulus can be estimated from equation (1) as the value at which the average tension $\langle T\rangle = 12\,\mathrm{nN}$, i.e. $E = (\langle kl\rangle - 17\langle T\rangle)/\langle 32wt^3/l^2\rangle = 0.43\,\mathrm{TPa}$.

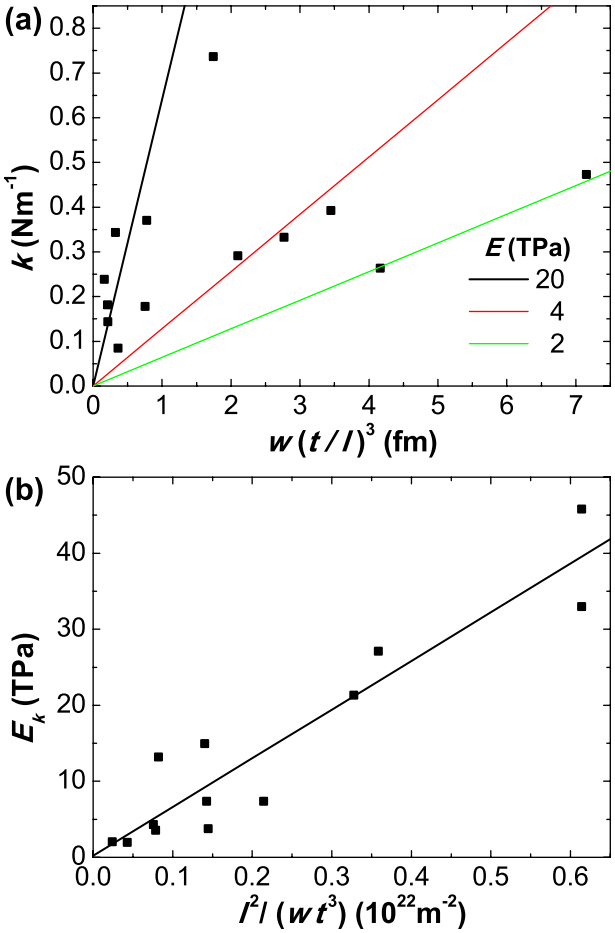

Figure 5. Experimental values for elastic constants of suspended graphene sheets. (a) Elastic constant k as a function of sheet dimensions represented by a quantity $w(t/l)^3$. The experimental data do not follow the linear fit (plotted for three different values of elastic modulus) expected in the limit of vanishing tension. (b) Scaled elastic modulus $E_k = kl^3/(32wt^3)$ as a function of sheet dimensions can be fitted to a linear function.

Variations in tension and elastic modulus and differences in E from recently reported values $E = 0.5$–1 TPa [3, 14] are a consequence of the fabrication of the devices rather than experimental errors. Firstly, anisotropy of graphene leads to different values of elastic constants depending on the crystallographic orientation of graphene with respect to the PMMA windows. Secondly, numerical constants in equation (1) are very sensitive to slight changes in clamping conditions and point load configuration and can result in differences in the calculated elastic modulus of up to a factor of two [13]–[15]. Thirdly, calculated values of elastic constants depend on the exact thickness of monolayer graphene; here, the interlayer spacing in graphite was used. Fourthly, small resist residue stuck at certain points on the sheets can slightly alter their thickness locally, giving rise to some scattering.

The obtained tension $T = 12$ nN is at least one order of magnitude less than the tension in graphene sheets exfoliated on an SiO_2 substrate [7, 14] and comparable to that of reduced graphene oxide sheets deposited from aqueous solution [10]. Such a low tension can be

attributed to the relaxation of sheets during processing of the top PMMA layer. Consequent baking and cooling of the sample lead to the expansion and retraction of the PMMA layers and sheet (which have opposite thermal expansion coefficients) reducing the built-in tension [16]. Since built-in tension can significantly alter the resonant frequency of a beam it is of the utmost importance in the fabrication of NEMS to use a structure with low built-in tension, so that its properties are not modified.

4. Conclusion

Free-standing graphene sheets were fabricated by patterning windows in a double-layered PMMA stack in which graphene was sandwiched between the layers. The reported procedure results in partially relaxed suspended graphene sheets with built-in tensions more than one order of magnitude smaller than in mechanically exfoliated suspended sheets deposited on a conventional SiO_2 substrate. Low tension and high stiffness of fabricated free-standing graphene structures will enable the realization of reliable graphene NEMS resonators operating in the gigahertz range.

References

[1] Novoselov K S, Geim A K, Morozov S V, Jiang D, Zhang Y, Dubonos S V, Grigorieva I V and Firsov A A 2004 *Science* **306** 666–9
[2] Castro Neto A H, Guinea F, Peres N M R, Novoselov K S and Geim A K 2009 *Rev. Mod. Phys.* **81** 109–62
[3] Lee C, Wei X, Kysar J W and Hone J 2008 *Science* **321** 385–8
[4] Bolotin K I, Sikes K J, Jiang Z, Klima M, Fudenberg G, Hone J, Kim P and Stormer H L 2008 *Solid State Commun.* **146** 351–5
[5] Ekinci K L and Roukes M L 2005 *Rev. Sci. Instrum.* **76** 061101
[6] Bunch J S, van der Zande A M, Verbridge S S, Frank I W, Tanenbaum D M, Parpia J M, Craighead H G and McEuen P L 2007 *Science* **315** 490–3
[7] Poot M and van der Zant H S J 2008 *Appl. Phys. Lett.* **92** 063111
[8] Garcia-Sanchez D, van der Zande A M, Paulo A S, Lassagne B, McEuen P L and Bachtold A 2008 *Nano Lett.* **8** 1399–403
[9] Du X, Skachko I, Barker A and Andrei E Y 2008 *Nat. Nanotechnol.* **3** 491–5
[10] Gómez-Navarro C, Burghard M and Kern K 2008 *Nano Lett.* **8** 2045–9
[11] Ferrari A C *et al* 2006 *Phys. Rev. Lett.* **97** 187401
[12] Sader J E, Chon J W M and Mulvaney P 1999 *Rev. Sci. Instrum.* **70** 3967–9
[13] Gere J M and Timoshenko S P 1990 *Mechanics of Materials* (Boston: PWS-Kent)
[14] Frank I W, Tanenbaum D M, van der Zande A M and McEuen P L 2007 *J. Vac. Sci. Technol.* B **25** 2558–61
[15] Landau L D and Lifshitz E M 1986 *Theory of Elasticity* (Oxford: Butterworth-Heinemann)
[16] Bao W, Miao F, Chen Z, Zhang H, Jang W, Dames C and Lau C N 2009 *Nat. Nanotechnol.* **4** 562–6